J. Astrophys. Astr. (1984) 5, 149–158

Brightness, Polarization and Electron Density of the Solar Corona of 1980 February 16

K. R. Sivaraman, M. Jayachandran, K. K. Scaria, G. S. D. Babu, S. P. Bagare & A. P. Jayarajan *Indian Institute of Astrophysics, Bangalore 560034*

Received 1983 September 1; accepted 1984 January 30

Abstract. During the eclipse of 1980 February 16 we photographed the solar corona at an effective wavelength of 6300 Å. Using a quadruple camera we also obtained the coronal pictures in polarized light for four polaroid orientations. We have used these observations to derive the coronal brightness and polarization and from these the electron densities in the corona out to a distance of about 2.5 $R_\odot$ from the centre of the disc. The coronal brightness matches well with that of the corona of 1958 October 12.

Key words: solar eclipse—solar corona: brightness, polarization, electron density

1. Introduction

The solar eclipse of 1980 February 16, with its belt of totality within 800 km of Bangalore, made it possible to conduct several experiments for the study of the solar chromosphere and corona. Two camps were set up, one at Hosur about 40 km south of Hubli and a second one at the state central farm at Jawalgere about 50 km east of Raichur.

The long-focus camera for the broad-band photography of the corona, the polarigraph and a coronal spectrograph were located at the camp at Hosur (latitude 15° 00′ 12″ N; longitude $5^h\,00^m\,36.3^s$ E) about 4 km south of the central line of totality. The duration of totality at the site was 164 s. The second contact was predicted at $10^h\,13^m\,9.0^s$ U.T. The skies were clear many days before and on the eclipse day and the winds were exceptionally low. In this paper we present the results obtained from the polarigraph and the coronal photographs with the long-focus camera.

2. The observations

2.1 *Broad-band Photometry*

We photographed the corona through a broad-band filter with peak transmission around 6300 Å (Wratten 25) using the same arrangement as during the eclipse of 1970 March 7 at Mexico (Bappu, Bhattacharyya & Sivaraman 1973). This consisted essentially of an $f/48$, 6.0-m focal length camera fed by a siderostat of 30 cm aperture

Table 1. Details of the exposures of the broad-band coronal photographs.

Plate No.	Duration of exposure s	Developer
1	Instantaneous	Promicrol
2	2	Promicrol
3	10	Promicrol
4	30	Promicrol
5	50	Promicrol diluted

and a rotating plate holder that accommodated six 8 × 10 inch plates of Kodak IIIa-F emulsion. The shutter of the camera located in front of the objective was operated from the focal plane end by the observer who changed the plate after each exposure in a pre-programmed sequence. The scheme of these exposures are set out in Table 1. Photometric standards were impressed on plates belonging to the same box of IIIa-F emulsion in the laboratory with a Kodak step-wedge with eleven steps, their densities ranging from 0.86 to 3.08. The exposures with the standard wedge of the same duration as for the eclipsed Sun established a relative photometric scale. This in turn was related to the mean brightness of the solar disc through exposures of the disc made on the day after the eclipse around the same time, through a Kodak neutral-density filter of density 4.7 and a 12.7 mm diameter diaphragm over the objective. Each photograph was processed along with its step-wedge calibration and the absolute calibration plates, details of which are also presented in Table 1.

2.2 *The Polarigraph*

The experiment designed to record the polarization of the corona from the limb to about $3R_\odot$ was carried out with a quadruple lens camera with identical Zeiss lenses of

Table 2. Details of the exposures with the quadruple lens polarigraph.

Exposure No.	Duration of exposure s	Frame number in each exposure for the four polaroid positions			
		A ↔	*B* ⤡	*C* ↕	*D* ⤢
1	Instantaneous	1	2	3	4
2	1	5	6	7	8
3	2	9	10	11	12
4	4	13	14	15	16
5	6	17	18	19	20
6	12	21	22	23	24
7	20	25	26	27	28
8	Instantaneous	29	30	31	32
9	1	33	34	35	36
10	3	37	38	39	40
11	5	41	42	43	44
12*	7	45	46	47	48

*Diamond Ring appeared.

1 m focal length working at $f/10$ and supported on an equatorial mount. Four polarizers cut from the same sheet of HN 32 polaroid together with four Wratten 25 Kodak gelatine filters were mounted near the focal plane such that the axis of each of the polaroids was inclined at 45° with reference to its neighbour. The four polarized images of the corona were photographed in one shot of exposure on 70-mm Kodak 2485 film. This film in 150-foot roll was mounted in the film transport of the camera so that the entire sequence of exposures planned during the progress of the eclipse could be photographed without any interruption. One member of the team operated the shutter and another the film transport.

In Table 2 we present the details of the exposures made after the announcement of the second contact in the camp. The impression of the standard wedge was established on that part of the film in the same roll which remained unused after the exposures during the eclipse. The entire film roll was developed in a developing tank, a few days after the eclipse.

3. Reductions and results

3.1 *Absolute Surface Brightness*

Among the five broad-band photographs obtained within the high-resolution image, the 10-s and 30-s exposures were chosen for evaluating the surface brightness distribution in the corona. We derived the isophotes by the equidensitometry technique

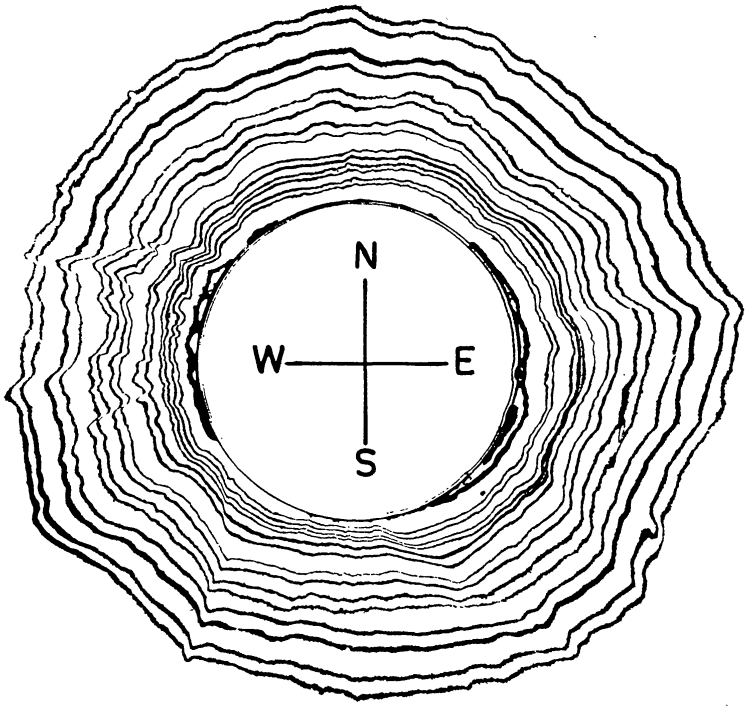

Figure 1. Isophotes of the solar corona. The outermost isophote is 1 and the numbers increase towards the solar limb (see Table 3).

based on the Sabattier effect, which has been employed with considerable success earlier (Bappu, Bhattacharyya, & Sivaraman 1973), using the high contrast Indu Graphic Arts film. We made the final composite by combining together the family of contours of each plate. The two plates had two of their density contours common between them. By perfectly overlapping these common density contours we ensured the matching of the rest of the isophotes of one plate with those of the other. The composite thus derived and shown in Fig. 1 has isophotes running from 1.01 to $2.53R_\odot$ from the centre of the Sun.

To obtain the intensity gradients along the polar and equatorial directions, we made microdensitometer scans along the two diameters approximately at position angles 0°, 90°, 180° and 270° and derived the intensity values on a relative scale using the step-wedge calibration curve. The mean of the four values represented the intensity level of each of the isophotes on an arbitrary photometric scale. We then transformed these intensities from the relative scale to values expressed in terms of the mean brightness of the solar disc $\bar{B}_\odot$ using the absolute calibration, adopting the value $\bar{B}_\odot = 1.98 \times 10^5$ stilb outside the Earth's atmosphere (Allen 1973).

We have estimated the brightness level of the sky contribution from traces made diagonally from one end of the plate to the other across the moon. The sky brightness at about $5R_\odot$ has a value of 1.5×10^{-10} of average brightness of the solar disc. In Table 3 we give the intensities of the isophotes in units of 10^{-8} of the mean brightness of the solar disc after correction for the sky brightness. The brightness of the corona along the N, S, E, W are represented in Fig. 2 and those along the equatorial and polar diameters in Fig. 3. Waldmeier's values of the brightness of the corona of 1958 October 12 along the same directions, extracted from the compilations of Hata & Saito (1966) are also shown in Fig. 3 for comparison. It is interesting to note the close agreement between our present values and those of Waldmeier in view of the fact that both these eclipses

Table 3. Intensities in the equatorial direction (mean of east and west) of the corona of 1980 February 16.

Isophote No.	$r/R_\odot$*	$B/\bar{B}_\odot$†
1	2.244	6.59
2	2.148	7.45
3	1.973	9.86
4	1.882	11.84
5	1.747	16.57
6	1.690	19.99
7	1.591	30.26
8	1.536	41.32
9	1.433	79.83
10	1.380	110.49
11	1.332	151.55
12	1.294	184.02
13	1.223	264.57
14	1.188	329.41

* Equatorial radius in the units of solar radius.
† Intensities in the units of 10^{-8} times the mean brightness of the solar disc.

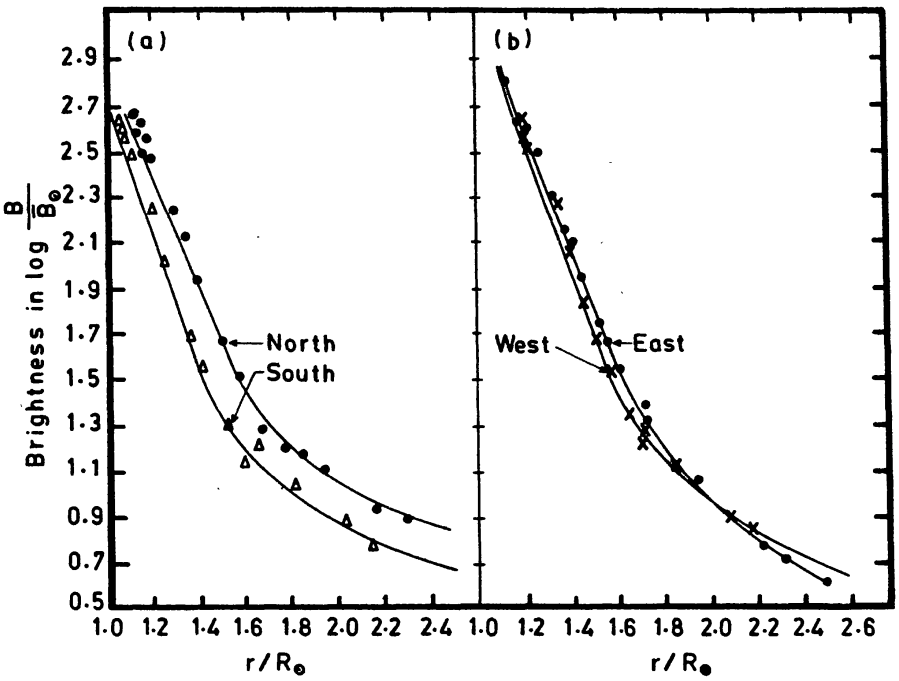

Figure 2. Brightness of the corona $(K+F)$ along the north (filled circles), south (open triangles), east (filled circles) and west (crosses) directions, expressed in units of 10^{-8} of the mean brightness of the solar disc $(\overline{B}_\odot)$, corrected for sky brightness. The curves represent the 19th-degree polynomial fit.

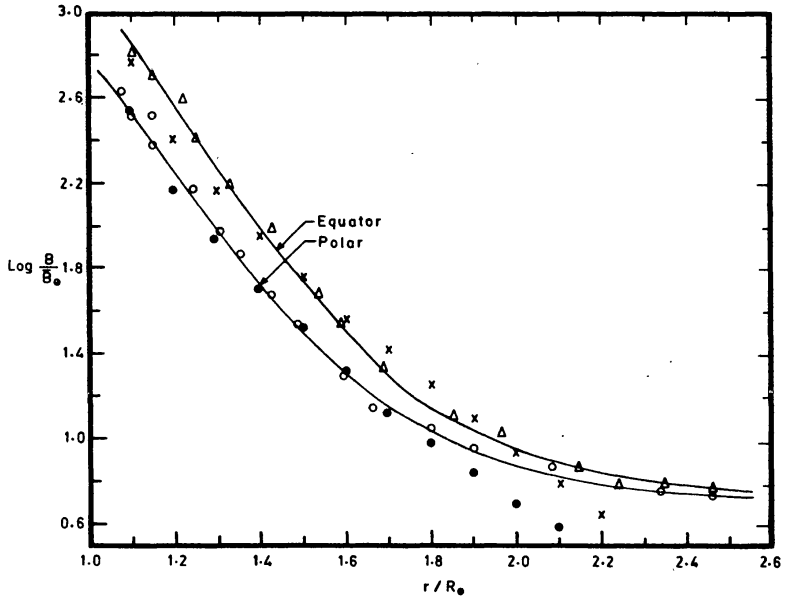

Figure 3. Brightness of the corona $(K+F)$ along the equatorial and polar diameters. The curves represent the 19th-degree polynomial fit to the observed points (open triangles and open circles). Waldmeier's results (crosses and filled circles) for the corona of 1958 October 12 eclipse are plotted for comparison.

occurred at epochs of two of the most prominent maxima of solar activity. The radial brightness distribution along the equatorial and polar directions can be represented by a polynomial of the form

$$B = \sum C_n r^{-n}. \tag{1}$$

By numerous trials using various degrees of polynomials starting from the 30th degree and employing the method of least squares we determined the polynomials representing the best fit with our observations. We find that only the coefficients listed below are significant and by the addition of the intermediate terms the quality of the fit does not improve.

Equatorial:

$$\frac{B_{eq}}{\bar{B}_\odot} = -\frac{0.21\times10^7}{r^{19}} + \frac{0.83\times10^7}{r^{17}} - \frac{0.14\times10^8}{r^{15}} + \frac{0.13\times10^8}{r^{13}} - \frac{0.78\times10^7}{r^{11}} + \frac{0.28\times10^7}{r^9} - \frac{0.62\times10^6}{r^7} + \frac{0.75\times10^5}{r^5} - \frac{0.37\times10^4}{r^3} \tag{2}$$

Polar:

$$\frac{B_{polar}}{\bar{B}_\odot} = \frac{0.10\times10^7}{r^{19}} - \frac{0.45\times10^7}{r^{17}} + \frac{0.83\times10^7}{r^{15}} - \frac{0.84\times10^7}{r^{13}} + \frac{0.52\times10^7}{r^{11}} - \frac{0.19\times10^7}{r^9} + \frac{0.44\times10^6}{r^7} - \frac{0.54\times10^5}{r^5} + \frac{0.29\times10^4}{r^3} \tag{3}$$

These polynomial curves are also shown in Fig. 2. The above coefficients are optimum for the best fit possible. The mean departure we have tolerated between the observations and the polynomial fit is 10 per cent for $r/R_\odot \leqslant 1.5$ and 5 per cent for $r/R_\odot > 1.5$. J. Dürst (1981, personal communication) has confirmed that such a polynomial as above represents very well the brightness distribution in the corona.

3.2 *Polarization*

From the data secured, exposures 1, 2, 3 and 10 were considered most worthy of future analysis. The 12-s exposure shows the weak contribution from the sky background which increases rapidly in higher exposures. We designate the four images through the polaroids as A, B, C and D, the first one having its electric vector parallel to the polar axis of the Sun and the subsequent ones in steps of 45° with reference to A. The light from the corona is linearly polarized due to Thomson scattering and can be divided into two orthogonal components characterised by a maximum and a minimum. If this maximum intensity makes an angle θ with the direction of the electric vector of A, then for each point in the corona the polarization P and the position angle θ can be computed from the standard relations,

$$P = \left[\left(\frac{A-C}{A+C}\right)^2 + \left(\frac{B-D}{B+D}\right)^2\right]^{\frac{1}{2}}, \tag{4}$$

$$\theta = \tan^{-1}\left(\frac{B-D}{A-C}\right). \tag{5}$$

The films were scanned using the PDS microdensitometer system at the Kitt Peak National Observatory by one of us (K.R.S) with a 100-μm square aperture. For each polarized image, the digitised output of the microdensitometer consisted of a 320 × 320 term matrix. These were found to be highly resolved and hence five consecutive density values were block averaged and converted into an array of 64 × 64 points of relative intensity values. Such four arrays derived from the four images corresponding to the four orientations of the polaroids, belonging to one exposure were now combined according to Equation (4) and the polarization values in per cent were computed point by point. Even a small error in the assignment of position angles would introduce local differences between the four measures. We have taken extreme care in marking the N-S and E-W fiducial directions on each of the images using their enlarged transparencies and then transferring these onto the originals. While adopting this procedure we ensured that the misalignment errors in the orientations among the 4 images did not exceed 1°.

We repeated the above analysis for three more sets of exposures. The agreement between the four sets are so good (within 10 per cent) that we derived the mean values of

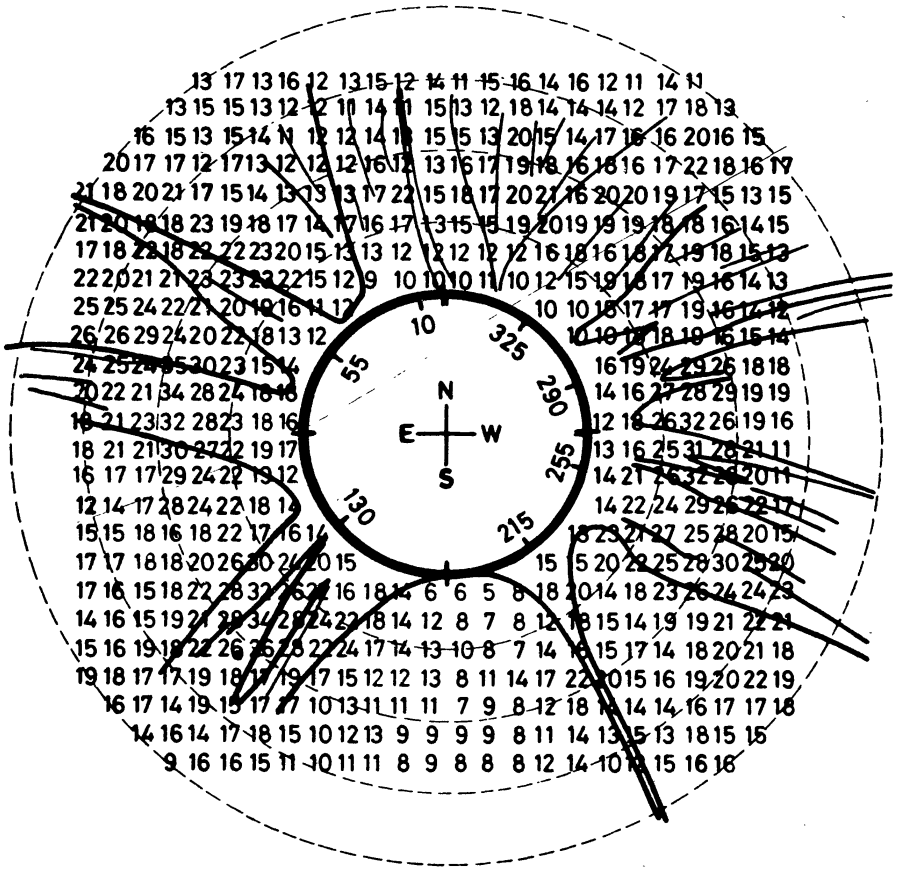

Figure 4. Polarization $P(K+F)$ of the corona. Each number represents the polarization in per cent over an area of 3.3 (arcmin)^2. Superposed is a schematic representation to scale of the coronal streamers. Notice the very low polarization near the south. The four circles in dashed lines represent the radial distances in terms of the solar radius ($r/R_\odot$ = 1.5, 2.0, 2.5 and 3.0) from the Sun's centre.

polarization point by point from the four sets. To measure the sky light we made tracings on every film diagonally across and reaching upto 8 solar radii from the centre of the moon. The mean sky brightness from each set of exposures has values around $4.5 \times 10^{-10} \bar{B}_{\odot}$. The mean value of the sky polarization was found to be 0.055 and inclination 7° to the vertical. The polarization values derived for the corona are those after correction for the sky polarization for the respective sets of exposures. Since the neighbouring values of polarization in the 64×64 configuration were almost identical over most part of the corona, we once again averaged the polarization to obtain a 32×32 matrix formation. Thus each value of the polarization represents the mean over a fictitious aperture of area 1000 μm × 1000 μm corresponding to 200 square arcsec on the corona. These mean polarization values are presented in Fig. 4. On these are superposed a schematic scale representation of the coronal features to enable identification of the prominent coronal features and the polarization values associated with them. The angles of deviation of the magnetic vector from the radial direction were also computed and it was found that the maximum departure from the radial direction does not exceed $\pm 8°$.

3.3 *Electron Density*

Our observations provide the intensity and polarization of the combined K and F corona represented by $(K+F)$ and P_{K+F} respectively at 32×32 points within the corona. We have used these to separate the K and F components in the customary way and have calculated the electron densities $N_e(r)$ of the K corona. If we assume that the polarization of the F component is zero for the distances involved in our observations, then these quantities are related to the unknown quantity (K), the intensity of the K corona and the polarization P_K of the K corona alone by the relation

$$\frac{P_{K+F}}{P_K} = \frac{K}{K+F}. \tag{6}$$

Following the procedure adopted by von Klüber (1958) we computed

$$K_t - K_r = K P_K = (K+F) P_{K+F} \tag{7}$$

where the subscripts t and r denote the tangential and radial intensity components of K. $K_t - K_r$ can be represented by a power series of the form

$$K_t - K_r = \sum_s h_s r^{-s} \tag{8}$$

where r is the apparent distance of a given point from the centre of the Sun in the units of solar radius. The electron density can then be expressed by a power series of the form

$$N_e(r) = \sum_s \frac{h_s}{a_{s+1}} \cdot \frac{1}{r^{s+1}} \cdot \frac{1}{C} \cdot \frac{1}{A(r) - B(r)}. \tag{9}$$

Using the intensity values at every 10° interval in position angles derived from the isophotes, along with the polarization values at the corresponding points, we have computed the values of $N_e(r)$ using the relation (9). We adopted the value $C = 3.44 \times 10^{-6}$ cm^3 and the values of a_s, $A(r)$ and $B(r)$ appropriate for the limb-darkening coefficient $q = 0.75$, from the compilations of van de Hulst (1950). In Fig. 5 we present the values of $N_e(r)$ so derived over the entire corona at every 10° in position angle. The

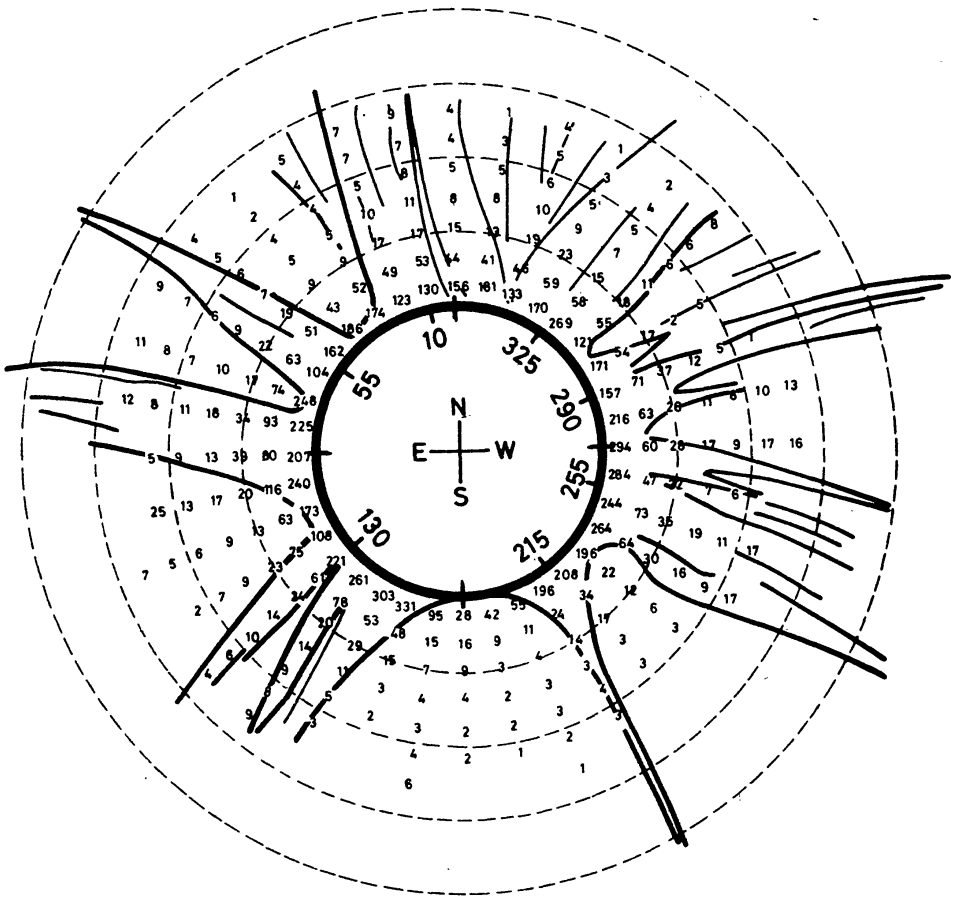

Figure 5. Distribution of the electron density $N_e(\mathrm{cm}^{-3})$, in units of 10^{-7}, in the corona of 1980 February 16. The four dashed circles are at the radii $r/R_\odot$ = 1.5, 2.0, 2.5 and 3.0, respectively, from the centre of the Sun.

electron densities along N, S, E and W directions are plotted in Fig. 6. Dürst (1982) has derived the electron densities, representative of the mean background corona by averaging the values for 8 position angles free of coronal holes or streamers for the same eclipse. We find that a plot of these values included in Fig. 6, lies midway between our curves for the north and the equatorial directions. This brings out the agreement between the two independent observations of the same eclipse. The bright streamers have electron densities in the range 3.5–4.0 $\times$ 10^7 cm^{-3} at 1.5$R_\odot$, while the region in the south between position angles 170° and 190° has extraordinarily low values in the range 3.5–6.0 $\times$ 10^6 cm^{-3} similar to those in a coronal hole. In Fig. 6 the enhancement of N_e beyond 2.0 $R_\odot$ in the west, is caused by the streamer in this direction. The presence of such enhancements due to streamers have been illustrated well by Dollfus, Laffineur & Mouradian (1974) in their study of the electron density models of streamers. The brightness enhancement due to this streamer can also be identified in the brightness gradient curve in the west direction beyond 2.0 $R_\odot$ in Fig. 2.

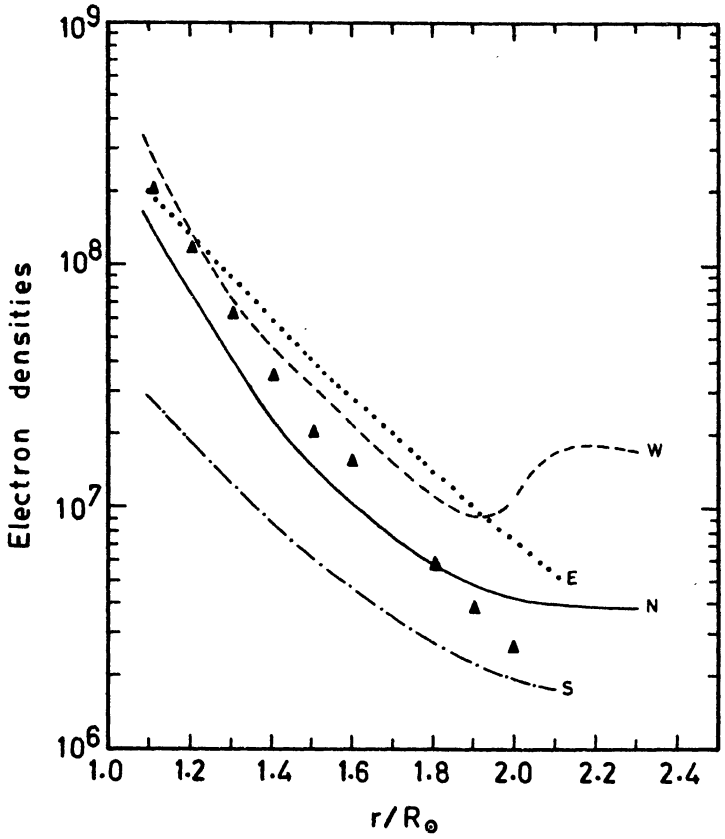

Figure 6. Electron density in the corona along the north, south, east and west directions. The electron density values of Dürst (filled triangles) for the same eclipse are also plotted for comparison. Notice the enhancement of N_e in the west at $r/R_\odot \sim 2$ due to a strong streamer.

Acknowledgements

The authors wish to thank the late Dr M. K. V. Bappu who was responsible for creating all the facilities for setting up these experiements. K.R.S. is thankful to Dr J. Dürst—formerly with the Institut für Astronomie, ETH Zentrum Zürich—for very valuable discussions during the latter's visit to India in January 1981. K.R.S. also wishes to express his gratitude to Mr Charles Mahaffey of the Kitt Peak National Observatory, Tucson, for his valuable help at the PDS microdensitometer system and in computations with the Cyber at KPNO. We are also thankful to Mr P. M. S. Namboodiri who helped us with the electron density computations.

References

Allen, C. W. 1973, *Astrophysical Quantities*, 3 edn, Athlone Press, London.
Bappu, M. K. V., Bhattacharyya, J. C., Sivaraman, K. R. 1973, *Pramana*, **1**, 117.
Dollfus, A., Laffineur, M., Mouradian, Z. 1974, *Solar Phys.*, **37**, 367.
Dürst, J. 1982, *Astr. Astrophys.*, **112**, 241.
Hata, S., Saito, K. 1966, *Ann. Tokyo astr. Obs.*, Ser. 2, **10**, 16.
van de Hulst, H. C. 1950, *Bull. astr. Inst. Netherl.*, **11**, 135.
von Klüber, H. 1958, *Mon. Not. R. astr. Soc.*, **118**, 201.
Waldmeier, M. 1959, *Z. Astrophys.*, **48**, 9.